

Balancing High Thermal Stability with High Activity in Diaryliminoacenaphthene-Nickel(II) Catalysts for Ethylene Polymerization

Yanjun Chen,^{a,b} Shizhen Du,^b Chuanbing Huang,^b Gregory A. Solan,^{*,b,c} Xiang Hao^b and Wen-Hua Sun^{*,b,d}

(Yanjun Chen and Shizhen Du made an equal contribution in this paper).

^aDepartment of Applied Chemical Engineering, Ningbo Polytechnic, Ningbo, 315800, China

^bKey Laboratory of Engineering Plastics and Beijing National Laboratory for Molecular Sciences, Institute of Chemistry, Chinese Academy of Sciences, Beijing 100190, China.

^cDepartment of Chemistry, University of Leicester, University Road, Leicester LE1 7RH, UK.

^dState Key Laboratory for Oxo Synthesis and Selective Oxidation, Lanzhou Institute of Chemical Physics, Chinese Academy of Sciences, Lanzhou 730000, China.

Correspondence to: W.-H. Sun (E-mail: whsun@iccas.ac.cn) or G. A. Solan (E-mail: gas8@leicester.ac.uk)

ABSTRACT: The *N,N*-diaryliminoacenaphthenes, 1,2-[2,4-[(4-FC₆H₄)₂CH]₂-6-MeC₆H₄N]₂-C₂C₁₀H₆ (**L1**) and 1-[2,4-[(4-FC₆H₄)₂CH]₂-6-MeC₆H₄N]-2-(ArN)C₂C₁₀H₆ (Ar = 2,6-Me₂C₆H₃ **L2**, 2,6-Et₂C₆H₃ **L3**, 2,6-*i*-Pr₂C₆H₃ **L4**, 2,4,6-Me₃C₆H₂ **L5**, 2,6-Et₂-4-MeC₆H₂ **L6**), incorporating at least one *N*-2,4-bis(difluorobenzhydryl)-6-methylphenyl group, have been synthesized and fully characterized. Interaction of **L1** – **L6** with (DME)NiBr₂ (DME = 1,2-dimethoxyethane) generates the corresponding nickel(II) bromide *N,N*-chelates, LNiBr₂ (**1** – **6**), in high yield. The molecular structures of **3** and **6** reveal distorted tetrahedral geometries at nickel with the *ortho*-substituted difluorobenzhydryl group providing enhanced steric protection to only one side of the metal center. On activation with various aluminium alkyl co-catalysts, such as MAO or Et₂AlCl, **1** – **6** displayed outstanding activity towards ethylene polymerization (up to 1.02 × 10⁷ g of PE (mol of Ni)⁻¹ h⁻¹). Notably **1**, bearing equivalent fluorobenzhydryl-substituted *N*-aryl groups, was able in the presence of Et₂AlCl to couple high activity with exceptional thermal stability generating high molecular weight branched polyethylenes at temperatures as high as 100 °C.

KEYWORDS: Nickel complex; cationic polymerization; polyethylene; branched; thermal properties

INTRODUCTION

The disclosure of nickel- and palladium-based α -diimine complexes as olefin polymerization catalysts by Brookhart and

co-workers more than twenty years ago represents a key milestone in the field.¹ Since then, considerable attention has been focused on the design and development of

other highly active late transition metal homogeneous olefin polymerization catalysts.² Although the early α -diimine systems exhibited high activities and a tolerance for the incorporation of polar olefins, their poor thermal stability at elevated temperature has hindered their industrial application; operating temperatures of between 80 to 100 °C being common.³ To overcome this limitation, various efforts have been made to improve the thermal stability of Ni and Pd α -diimine catalysts, such as variations of the substituents on the imino-aryl groups, right through to modifications of the ligand backbone itself. For example, the cyclophane-containing diimine Ni and Pd catalysts reported by Guan exhibit high turnover frequencies and enhanced thermal stability for ethylene polymerization,⁴ while the Ni α -diimine catalysts bearing camphorquinone-based ligands described by Gao display reasonable thermal stability.⁵ Elsewhere, *N,N*-frameworks bearing bulky benzhydryl-derived substituents have started to emerge in polymerization applications, and indeed these substituents, if judiciously positioned, have been shown to sterically protect the active nickel species by impeding *N*-aryl group rotations thereby enhancing the thermal stability of the catalyst.^{6–10} As part of our on-going research program directed towards the development of ligand sets incorporating this CH(Ph)₂ group, we have found that nickel catalysts bearing 2-bis(arylimino) acenaphthenes,⁷ 2-(aryliminomethyl) pyridines⁸ and 2,3-bis(arylimino)butane derivatives all benefit from improved thermal stability.⁹ More recently, some thermally robust Ni and Pd α -diimine catalysts that incorporate 2,6-dibenzhydryl-4-methylphenyl as the *N*-aryl groups (*e.g.*, **A**, Chart 1) have also shown great promise in ethylene polymerization applications.¹⁰ However, while such 2,6-disubstituted bulky groups have the effect of enhancing the thermal stability, this tends to be at the expense of lowering the catalytic activity; an observation that can be attributed to their steric hindrance to insertion of ethylene into the Ni-C/H bond of the active species.^{3b}

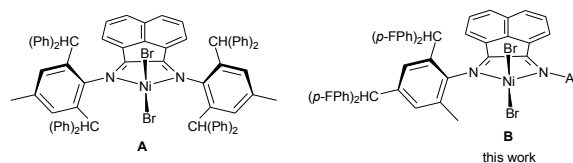


CHART 1 Evolution of benzhydryl-substituted diaryliminoacenaphthene-nickel pre-catalysts

With a view to developing a nickel catalyst that can couple more effectively good thermal stability with high activity, we report our findings at developing diaryliminoacenaphthene-nickel precatalysts that contain a fluorinated benzhydryl group at only one of the *ortho*-sites of the *N*-aryl group and a methyl group at the other (**B**, Chart 1).

We reasoned that by reducing the steric properties of the second *ortho* group, access to the active Ni center by the ethylene monomer would be increased leading to a more active catalyst, but without compromising on thermal stability imparted by the presence of a substituted benzhydryl group. In other work we have shown that the introduction of *para*-fluorine groups can have advantageous effects on catalytic activity and have hence modified the benzhydryl group accordingly.^{11,12} Specifically we disclose an in-depth evaluation of the catalytic performance of both symmetrical, [1,2-[2,4-((4-FC₆H₄)₂CH)₂-6-MeC₆H₄N]₂-C₂C₁₀H₆]NiBr₂, as well as a range of unsymmetrical, [1-[2,4-((4-FC₆H₄)₂CH)₂-6-MeC₆H₄N]-2-(ArN)C₂C₁₀H₆]NiBr₂ (Ar = 2,6-Me₂C₆H₃, 2,6-Et₂C₆H₃, 2,6-*i*-Pr₂C₆H₃, 2,4,6-Me₃C₆H₂, 2,6-Et₂-4-MeC₆H₂), examples of **B** as precatalysts for the polymerization of ethylene. Notably, some unique and quite surprising observations are made, such as high catalytic activities (up to 8.52 × 10⁶ g of PE (mol of Ni)⁻¹ h⁻¹), exceptional thermal stability (with activity of 1.12 × 10⁶ g of PE (mol of Ni)⁻¹ h⁻¹ at 100 °C), while generating high molecular weight polyethylenes (up to 10⁵ g mol⁻¹) at elevated reaction temperature.

EXPERIMENTAL

All manipulations involving air- and moisture-sensitive compounds were carried out under a nitrogen atmosphere using standard Schlenk techniques. Toluene was refluxed over sodium and distilled under nitrogen prior to use. Methylaluminoxane (MAO, 1.46 M solution in toluene) and modified methylaluminoxane (MMAO, 2.00 M in heptane) were purchased from Akzo Nobel Corp. Diethylaluminium chloride (Et_2AlCl , 1.17 M in toluene), ethylaluminium dichloride (EtAlCl_2 , 1.00 M in toluene) and dimethylaluminium chloride (Me_2AlCl , 1.00 M in toluene) were purchased from Acros Chemicals. High-purity ethylene was purchased from Beijing Yansan Petrochemical Co. and used as received. Other reagents were purchased from Aldrich, Acros or local suppliers. NMR spectra were recorded on a Bruker DMX 400 MHz instrument at ambient temperature using TMS as an internal standard. IR spectra were recorded on a Perkin-Elmer System 2000 FT-IR spectrometer. Elemental analysis was carried out using a Flash EA 1112 micro-analyzer. Molecular weights and molecular weight distributions (MWD) of the polyethylenes were obtained using a PL-GPC220 instrument at 150 °C with 1,2,4-trichlorobenzene as the solvent. The melting points of the polyethylenes were measured from the second scanning run on a Perkin-Elmer TA-Q2000 differential scanning calorimetry (DSC) analyzer under a nitrogen atmosphere. In the procedure, a sample of about 4.0 mg was heated to 140 °C at a rate of 20 °C/min and kept for 2 min at 140 °C to remove the thermal history and then cooled at a rate of 20 °C/min to -40 °C. ^{13}C NMR spectra of the polyethylenes were recorded on a Bruker DMX 300 MHz instrument at 135 °C in deuterated 1,2-dichlorobenzene with TMS as an internal standard.

Preparation of the imine-ketone intermediate and ligands L1 - L6

2-[2,4-Bis(bis(4-fluorophenyl)methyl)-6-methylphenylimino]acenaphthylen-1-one. To a

mixture of CH_2Cl_2 (200 mL) and EtOH (10 mL), acenaphthylene-1,2-dione (3.643 g, 20 mmol) and 2,4-bis[bis(4-fluorophenyl)methyl]-6-methylbenzenamine (10.231 g, 20 mmol) were added. The mixture was stirred for 12 h at room temperature in the presence of a catalytic amount of *p*-toluenesulfonic acid. The volatiles were removed under reduced pressure and the residue was further purified by column chromatography on aluminium oxide using petroleum ether/ethyl acetate (V:V = 50:1) as the eluent affording the product as a red solid (7.663 g, 57%). Mp: 124–126 °C. ^1H -NMR (CDCl_3 , 400 MHz, TMS): δ 8.14–8.08 (m, 2H), 7.93 (d, J = 8.4 Hz, 1H), 7.78 (t, J = 7.6 Hz, 1H), 7.05–7.00 (m, 8H), 6.98–6.83 (m, 6H), 6.69–6.65 (m, 2H), 6.48 (s, 1H), 6.39 (d, J = 7.2 Hz, 1H), 6.10 (t, J = 8.4 Hz, 2H), 5.48 (s, 1H), 5.46 (s, 1H), 2.00 (s, 3H). ^{13}C NMR (CDCl_3 , 100 MHz, TMS): δ 189.5, 162.7, 161.6, 160.3, 160.1, 146.6, 142.6, 139.5, 132.6, 132.2, 131.0, 130.9, 130.7, 130.6, 130.5, 130.4, 130.2, 129.4, 128.5, 128.1, 127.5, 127.4, 125.0, 122.5, 122.0, 115.3, 115.1, 114.9, 114.7, 114.5, 114.3, 54.7, 50.8, 17.7. FT-IR (cm^{-1}): 3047 (w), 2956 (w), 2868 (w), 1730 (m), 1653 (u(C=N), m), 1600 (m), 1505 (s), 1221 (s), 1157 (s), 828 (s), 779 (s). Anal. Calc for $\text{C}_{45}\text{H}_{29}\text{F}_4\text{NO}$ (675.71): C, 79.99; H, 4.33; N, 2.07%. Found: C, 80.17; H, 4.20; N, 2.15%.

L1. Under an atmosphere of nitrogen, 2,4-bis[bis(4-fluorophenyl)methyl]-6-methylbenzenamine (1.023 g, 2.0 mmol) was dissolved in toluene (30 mL) and trimethylaluminum (2.0 mL, 1.0 M in toluene) added dropwise. The solution was stirred at reflux for 3 h before being allowed to cool to room temperature. A toluene solution of acenaphthylene-1,2-dione (0.182 g, 1.0 mmol) was added dropwise and the mixture stirred at reflux for 12 h. On cooling to room temperature the mixture was made alkali by the addition of aqueous NaOH (50%). The solution was extracted with CH_2Cl_2 (3 \times 20 mL) and the combined extracts dried over anhydrous MgSO_4 . Following filtration, the solvent was removed under reduced pressure to give an orange residue which was subject to chromatography on silica gel with petroleum

ether/ethyl acetate (V:V = 50:1) as eluent. **L1** was isolated as an orange solid (0.112 g, 8%). Mp: 160–162 °C. ^1H -NMR (CDCl_3 , 400 MHz, TMS): δ 7.75 (d, J = 7.6 Hz, 1H), 7.14 (t, J = 7.6 Hz, 1H), 7.08–6.96 (m, 8H), 6.92 (s, 1H), 6.83 (d, J = 7.2 Hz, 4H), 6.67–6.64 (m, 2H), 6.46 (s, 1H), 6.28 (d, J = 7.2 Hz, 1H), 5.98 (t, J = 7.6 Hz, 2H), 5.59 (s, 1H), 5.47 (s, 1H), 2.22 (s, 3H). ^{13}C NMR (CDCl_3 , 100 MHz, TMS): δ 163.1, 162.7, 161.5, 160.3, 160.1, 147.3, 139.7, 139.1, 138.6, 132.8, 131.0, 130.9, 130.7, 130.6, 130.5, 129.3, 129.0, 128.7, 128.6, 127.0, 125.4, 122.4, 115.3, 115.2, 115.0, 114.9, 114.7, 114.2, 114.0, 54.7, 50.9, 17.9. FT-IR (cm^{-1}): 3049 (w), 1659 ($\nu(\text{C}=\text{N})$, m), 1600 (m), 1503 (s), 1468 (w), 1221 (s), 1157 (s), 1095 (w), 1057 (w), 926 (w), 827 (s), 777 (s). Anal. Calc for $\text{C}_{78}\text{H}_{52}\text{F}_8\text{N}_2$ (1169.25): C, 80.12; H, 4.48; N, 2.40%. Found: C, 80.06; H, 4.27; N, 2.25%.

L2. 2-[2,4-bis(bis(4-fluorophenyl)methyl)-6-methylphenylimino]acenaphthylene-1-one (1.014 g, 1.5 mmol), 2,6-dimethylaniline (0.303 g, 2.5 mmol) and a catalytic amount of *p*-toluenesulfonic acid were dissolved in toluene (50 mL) and the mixture stirred at reflux for 8 h using a Dean-Stark apparatus. The resulting solution was then evaporated under reduced pressure and the residual solids further purified by column chromatography on aluminum oxide using petroleum ether/ethyl acetate (V:V = 50:1) as the eluent. **L2** was isolated as a yellow solid (0.492 g, 42%). Mp: 188–190 °C. ^1H NMR (CDCl_3 , 400 MHz, TMS): δ 7.83 (t, J = 8.8 Hz, 2H), 7.33 (t, J = 7.6 Hz, 1H), 7.21–7.11 (m, 3H), 7.07–6.99 (m, 9H), 6.97–6.78 (m, 7H), 6.10 (d, J = 7.2 Hz, 1H), 6.50 (s, 1H), 6.37 (d, J = 7.2 Hz, 1H), 6.16 (t, J = 8.4 Hz, 2H), 5.67 (s, 1H), 5.48 (s, 1H), 2.26 (s, 3H), 2.07 (s, 3H). ^{13}C NMR (CDCl_3 , 100 MHz, TMS): δ 162.7, 162.6, 162.5, 161.6, 161.1, 160.2, 160.1, 149.1, 147.4, 140.2, 139.8, 139.7, 138.9, 138.7, 137.3, 132.9, 131.2, 131.1, 130.7, 130.6, 130.5, 129.4, 129.1, 129.0, 128.9, 128.3, 128.1, 127.2, 125.4, 124.7, 123.9, 122.6, 122.3, 115.3, 115.2, 115.0, 114.9, 114.7, 114.4, 114.2, 54.7, 50.9, 18.2, 17.8, 17.7. FT-IR (cm^{-1}): 2979 (w), 2905 (w), 1676 ($\nu(\text{C}=\text{N})$, m), 1654 ($\nu(\text{C}=\text{N})$, m), 1598 (m), 1504 (s), 1466 (m), 1415 (m), 1221 (s), 1157 (m), 1074 (m), 1017 (m), 924 (m), 832 (s),

780 (s). Anal. Calc for $\text{C}_{53}\text{H}_{38}\text{F}_4\text{N}_2$ (778.88): C, 81.73; H, 4.92; N, 3.60%. Found: C, 81.66; H, 4.80; N, 3.52%.

L3. Using a similar procedure to that described for **L2** with 2,6-diethylaniline as the aniline, **L3** (0.530 g, 44%) was obtained as a yellow powder. Mp: 202–204 °C. ^1H NMR (CDCl_3 , 400 MHz, TMS): δ 7.81 (t, J = 8.4 Hz, 2H), 7.32 (t, J = 7.6 Hz, 1H), 7.25–7.15 (m, 4H), 7.09–6.97 (m, 8H), 6.92–6.78 (m, 7H), 6.59 (d, J = 7.2 Hz, 1H), 6.51 (s, 1H), 6.33 (d, J = 7.2 Hz, 1H), 6.16 (t, J = 8.4 Hz, 2H), 5.68 (s, 1H), 5.48 (s, 1H), 2.75–2.65 (m, 1H), 2.61–2.46 (m, 2H), 2.39–2.30 (m, 1H), 2.06 (s, 3H), 1.23 (t, J = 7.6 Hz, 3H), 1.06 (t, J = 7.6 Hz, 3H). ^{13}C NMR (CDCl_3 , 100 MHz, TMS): δ 162.7, 162.6, 161.6, 161.1, 160.2, 160.1, 159.2, 148.3, 147.4, 140.2, 139.8, 139.7, 138.9, 138.8, 132.9, 131.1, 130.8, 130.7, 130.6, 130.5, 129.4, 129.0, 128.9, 128.4, 127.9, 127.2, 126.5, 126.4, 125.4, 124.2, 122.8, 122.6, 115.2, 115.1, 115.0, 114.8, 114.6, 114.5, 114.3, 54.7, 50.9, 24.8, 24.6, 17.6, 14.5, 13.7. FT-IR (cm^{-1}): 2967 (w), 1671 ($\nu(\text{C}=\text{N})$, m), 1649 ($\nu(\text{C}=\text{N})$, m), 1599 (m), 1504 (s), 1463 (m), 1413 (m), 1223 (s), 1158 (m), 1090 (m), 1017 (m), 927 (m), 828 (s), 780 (s). Anal. Calc for $\text{C}_{55}\text{H}_{42}\text{F}_4\text{N}_2$ (806.93): C, 81.86; H, 5.25; N, 3.47%. Found: C, 81.69; H, 5.33; N, 3.39%.

L4. Using a similar procedure to that described for **L2** with 2,6-diisopropylaniline as the aniline, **L4** (0.577 g, 46%) was obtained as a yellow powder. Mp: 214–216 °C. ^1H NMR (CDCl_3 , 400 MHz, TMS): δ 7.80 (t, J = 8.0 Hz, 2H), 7.30–7.25 (m, 5H), 7.15 (t, J = 7.6 Hz, 1H), 7.09–6.97 (m, 8H), 6.92–6.52 (m, 7H), 6.55 (d, J = 7.2 Hz, 1H), 6.52 (s, 1H), 6.31 (d, J = 7.2 Hz, 1H), 6.15 (t, J = 8.4 Hz, 2H), 5.68 (s, 1H), 5.48 (s, 1H), 3.19–3.12 (m, 1H), 2.93–2.86 (m, 1H), 2.06 (s, 3H), 1.32 (d, J = 6.8 Hz, 3H), 1.20 (d, J = 6.8 Hz, 3H), 1.12 (d, J = 6.8 Hz, 3H), 0.87 (d, J = 6.8 Hz, 3H). ^{13}C NMR (CDCl_3 , 100 MHz, TMS): δ 162.7, 162.6, 161.6, 161.4, 160.3, 160.1, 159.2, 147.5, 147.1, 140.3, 139.8, 138.9, 138.8, 137.3, 135.4, 133.0, 131.1, 131.0, 130.7, 130.6, 130.5, 129.4, 129.0, 128.9, 128.8, 128.4, 127.7, 127.2, 125.4, 124.5, 123.7, 123.4, 123.2, 122.6, 115.2, 115.0, 114.8, 114.6, 114.5, 114.3, 54.7, 50.8, 28.7, 28.5, 23.8, 23.5,

23.3, 23.1, 17.6. FT-IR (cm^{-1}): 2965 (w), 1680 ($\nu(\text{C}=\text{N})$, m), 1653 ($\nu(\text{C}=\text{N})$, m), 1500 (m), 1505 (s), 1463 (m), 1437 (m), 1384 (w), 1226 (s), 1157 (m), 1091 (m), 1060 (m), 926 (m), 831 (s), 783 (s). Anal. Calc for $\text{C}_{57}\text{H}_{46}\text{F}_4\text{N}_2$ (834.98): C, 81.99; H, 5.55; N, 3.35%. Found: C, 81.72; H, 5.43; N, 3.34%.

L5. Using a similar procedure to that described for **L2** with 2,4,6-trimethylaniline as the aniline, **L5** (0.529 g, 45%) was obtained as a yellow powder. Mp: 204–206 °C. ^1H NMR (CDCl_3 , 400 MHz, TMS): δ 7.82 (t, J = 8.8 Hz, 2H), 7.35 (t, J = 7.6 Hz, 1H), 7.18 (t, J = 7.6 Hz, 1H), 7.09–6.98 (m, 10H), 6.92–6.78 (m, 7H), 6.68 (d, J = 7.2 Hz, 1H), 6.50 (s, 1H), 6.36 (d, J = 7.2 Hz, 1H), 6.15 (t, J = 8.4 Hz, 2H), 5.67 (s, 1H), 5.48 (s, 1H), 2.39 (s, 3H), 2.20 (s, 3H), 2.07 (s, 3H), 2.03 (s, 3H). ^{13}C NMR (CDCl_3 , 100 MHz, TMS): δ 162.7, 162.5, 161.6, 161.3, 160.2, 160.1, 159.2, 147.4, 146.6, 140.1, 139.8, 139.7, 138.8, 138.7, 137.4, 137.3, 133.1, 132.9, 131.2, 131.1, 130.7, 130.6, 130.5, 129.4, 129.2, 129.1, 129.0, 128.9, 128.4, 128.1, 127.2, 125.4, 124.5, 122.6, 122.3, 115.2, 115.0, 114.9, 114.6, 114.4, 114.2, 54.7, 50.9, 21.0, 18.1, 17.7, 17.6. FT-IR (cm^{-1}): 2972 (w), 1675 ($\nu(\text{C}=\text{N})$, m), 1651 ($\nu(\text{C}=\text{N})$, m), 1599 (m), 1507 (s), 1469 (m), 1418 (m), 1379 (m), 1222 (s), 1156 (m), 1093 (m), 1044 (m), 922 (m), 831 (s), 781 (s). Anal. Calc for $\text{C}_{54}\text{H}_{40}\text{F}_4\text{N}_2$ (792.90): C, 81.80; H, 5.08; N, 3.53%. Found: C, 81.68; H, 5.00; N, 3.41%.

L6. Using a similar procedure to that described for **L2** with 2,6-diethyl-4-methylaniline as the aniline, **L6** (0.579 g, 47%) was obtained as a yellow powder. Mp: 208–210 °C. ^1H NMR (CDCl_3 , 400 MHz, TMS): δ 7.81 (t, J = 8.4 Hz, 2H), 7.34 (t, J = 7.6 Hz, 1H), 7.16 (t, J = 7.9 Hz, 1H), 7.09–6.97 (m, 10H), 6.92–6.78 (m, 7H), 6.66 (d, J = 7.2 Hz, 1H), 6.51 (s, 1H), 6.32 (d, J = 7.2 Hz, 1H), 6.16 (t, J = 8.4 Hz, 2H), 5.68 (s, 1H), 5.48 (s, 1H), 2.70–2.61 (m, 1H), 2.57–2.44 (m, 2H), 2.43 (s, 3H), 2.36–2.22 (m, 1H), 2.06 (s, 3H), 1.21 (t, J = 7.6 Hz, 3H), 1.04 (t, J = 7.6 Hz, 3H). ^{13}C NMR (CDCl_3 , 100 MHz, TMS): δ 162.8, 162.7, 161.8, 161.4, 160.4, 160.2, 159.3, 147.6, 145.9, 140.3, 139.9, 138.9, 137.5, 133.5, 133.1, 131.3, 131.2, 130.9,

130.8, 130.7, 130.6, 130.5, 129.5, 129.2, 129.0, 128.6, 128.0, 127.4, 127.3, 125.5, 122.9, 122.7, 115.4, 115.2, 115.1, 115.0, 114.8, 114.6, 114.4, 54.9, 51.0, 24.9, 24.7, 21.3, 17.8, 14.7, 13.9. FT-IR (cm^{-1}): 2968 (w), 1671 ($\nu(\text{C}=\text{N})$, m), 1648 ($\nu(\text{C}=\text{N})$, m), 1599 (m), 1502 (s), 1461 (m), 1430 (m), 1378 (m), 1218 (s), 1156 (m), 1094 (m), 1018 (m), 924 (m), 829 (s), 779 (s). Anal. Calc for $\text{C}_{56}\text{H}_{44}\text{F}_4\text{N}_2$ (820.96): C, 81.93; H, 5.40; N, 3.41%. Found: C, 81.78; H, 5.32; N, 3.36%.

Preparation of 1 - 6

Complex 1. **L1** (0.245 g, 0.21 mmol) and (DME)NiBr₂ (0.062 g, 0.20 mmol) were dissolved in dichloromethane (10 mL) in a Schlenk tube and the mixture stirred for 12 h at room temperature. Excess diethyl ether was added, and the precipitate was collected by filtration, washed with diethyl ether, then dried under reduced pressure to obtain **1** as a deep red powder (0.173 g, 62%). FT-IR (cm^{-1}): 3048 (w), 1651 ($\nu(\text{C}=\text{N})$, w), 1601 ($\nu(\text{C}=\text{N})$, m), 1503 (m), 1469 (w), 1440 (w), 1294 (w), 1222 (s), 1157 (s), 1096 (m), 1044 (w), 1015 (w), 826 (s), 774 (s). Anal. Calc for $\text{C}_{78}\text{H}_{52}\text{F}_8\text{N}_2\text{NiBr}_2$ (1387.75): C, 67.51; H, 3.78; N, 2.02%. Found: C, 67.36; H, 3.50; N, 2.00%.

Complex 2. Using the method described for **1** above, with **L2** in place of **L1**, gave **2** as a deep red powder (0.177 g, 89%). FT-IR (cm^{-1}): 2923 (w), 1652 ($\nu(\text{C}=\text{N})$, w), 1627 ($\nu(\text{C}=\text{N})$, m), 1601 (m), 1504 (s), 1467 (m), 1441 (m), 1297 (m), 1219 (s), 1157 (m), 1094 (m), 1045 (w), 834 (s), 776 (s). Anal. Calc for $\text{C}_{53}\text{H}_{38}\text{F}_4\text{N}_2\text{NiBr}_2$ (997.38): C, 63.82; H, 3.84; N, 2.81%. Found: C, 63.53; H, 3.53; N, 2.86%.

Complex 3. Using the method described for **1** above, with **L3** in place of **L1**, gave **3** as a deep red powder (0.183 g, 89%). FT-IR (cm^{-1}): 2974 (w), 1663 ($\nu(\text{C}=\text{N})$, w), 1630 ($\nu(\text{C}=\text{N})$, m), 1598 (m), 1583 (m), 1504 (s), 1466 (m), 1439 (m), 1290 (m), 1221 (s), 1157 (m), 1094 (m), 1047 (w), 823 (s), 774 (s). Anal. Calc for $\text{C}_{55}\text{H}_{42}\text{F}_4\text{N}_2\text{NiBr}_2$ (1025.43): C, 64.42; H, 4.13; N, 2.73%. Found: C, 64.36; H, 4.01; N, 2.51%.

Complex 4. Using the method described for **1** above, with **L4** in place of **L1**, gave **4** as a deep red powder (0.191 g, 91%). FT-IR (cm^{-1}): 2967 (w), 1651 ($\nu(\text{C}=\text{N})$, w), 1624 ($\nu(\text{C}=\text{N})$, m), 1601 (m), 1505 (s), 1461 (m), 1437 (m), 1289 (m), 1223 (s), 1157 (m), 1097 (m), 1041 (m), 828 (s), 776 (s). Anal. Calc for $\text{C}_{57}\text{H}_{46}\text{F}_4\text{N}_2\text{NiBr}_2$ (1053.48): C, 64.99; H, 4.40; N, 2.66%. Found: C, 64.68; H, 4.13; N, 2.38%.

Complex 5. Using the method described for **1** above, with **L5** in place of **L1**, gave **5** as a deep red powder (0.177 g, 88%). FT-IR (cm^{-1}): 2915 (w), 1660 ($\nu(\text{C}=\text{N})$, w), 1629 ($\nu(\text{C}=\text{N})$, m), 1599 (m), 1576 (m), 1504 (s), 1471 (m), 1438 (m), 1292 (m), 1220 (s), 1154 (m), 1096 (m), 1044 (m), 824 (s), 773 (s). Anal. Calc for $\text{C}_{57}\text{H}_{46}\text{F}_4\text{N}_2\text{NiBr}_2$ (1011.40): C, 64.13; H, 3.99; N, 2.77%. Found: C, 63.95; H, 3.82; N, 2.56%.

Complex 6. Using the method described for **1** above, with **L6** in place of **L1**, gave **6** as a deep red powder (0.188 g, 90%). FT-IR (cm^{-1}): 2972 (w), 1648 ($\nu(\text{C}=\text{N})$, w), 1622 ($\nu(\text{C}=\text{N})$, m), 1599 (m), 1582 (m), 1504 (s), 1441 (m), 1414 (m), 1294 (m), 1223 (s), 1157 (m), 1095 (m), 1050 (m), 828 (s), 778 (s). Anal. Calc for $\text{C}_{57}\text{H}_{46}\text{F}_4\text{N}_2\text{NiBr}_2$ (1039.46): C, 64.71; H, 4.27; N, 2.70%. Found: C, 64.55; H, 4.12; N, 2.66%.

X-Ray structure determinations

Single-crystal X-ray diffraction studies for **3** and **6** was conducted on a Rigaku Sealed Tube CCD (Saturn 724+) diffractometer with graphite-monochromated Mo-K α radiation ($\lambda = 0.71073$ Å) at 173(2) K. Cell parameters were obtained by global refinement of the positions of all collected reflections. Intensities were corrected for Lorentz and polarization effects and empirical absorption. The structures were solved by direct methods and refined by full-matrix least-squares on F^2 . All non-hydrogen atoms were refined anisotropically and all hydrogen atoms were placed in calculated positions. Using the SHELXTL-97 package, structural solution and refinement were performed.¹³ In the structures of **3** and **6**, free solvent molecules which have no influence on

the geometry of the main compounds were obtained, and PLATON/SQUEEZE¹⁴ was used to remove these free solvents. Crystal data and processing parameters for **3** and **6** are summarized in Table 1. CCDC 1517298 (**3**) 1517299 (**6**) contain the crystallographic data for this article, which could be obtained free of charge from the Cambridge Crystallographic Data Centre via www.ccdc.cam.ac.uk/data_request/cif.

TABLE 1. Crystal data and structure refinement for **3** and **6**.

	3	6
Empirical formula	C ₅₅ H ₄₂ F ₄ N ₂ NiBr ₂	C ₅₆ H ₄₄ F ₄ N ₂ NiBr ₂
Mw	1025.44	1039.46
T (K)	173 (2)	173 (2)
Wavelength (Å)	0.71073	0.71073
Crystal system	Monoclinic	Monoclinic
Space group	P2(1)/c	P2(1)/n
a (Å)	15.419(3)	15.615(3)
b (Å)	17.906(4)	17.300(4)
c (Å)	19.183(4)	19.836(4)
α (°)	90	90
β (°)	112.56(3)	112.60(3)
γ (°)	90	90
V (Å ³)	4891.1(17)	4946.9(17)
Z	4	4
D calcd (mg m ⁻³)	1.393	1.396
μ (mm ⁻¹)	2.083	2.061
F (000)	2080	2112
Crystal size (mm)	0.36×0.18×0.11	0.41×0.14×0.08
θ range (°)	1.43–27.48	1.42–27.47
	–19 ≤ h ≤ 19	–19 ≤ h ≤ 20
Limiting indices	–23 ≤ k ≤ 23	–22 ≤ k ≤ 22
	–24 ≤ l ≤ 24	–25 ≤ l ≤ 25
No. of reflns collected	33245	33107
No. unique rflns [R(int)]	11157 (0.0609)	11254 (0.0682)
Completeness to θ (%)	99.6%	99.2 %
Absorption correction	Multi-scan	Multi-scan
Data/restraints/params	11157 / 0 / 580	11254 / 6 / 586
Goodness of fit on F ²	1.057	1.117
Final R indices [I >2σ(I)]	R1 = 0.1023, wR2 = 0.2642	R1 = 0.0766, wR2 = 0.1845
R indices (all data)	R1 = 0.1343, wR2 = 0.2916	R1 = 0.0961, wR2 = 0.1987
Largest diff peak and hole (e. Å ⁻³)	3.038 and - 0.841	1.377 and - 0.674

Polymerization studies

Ethylene polymerization at 1 atm ethylene pressure. The polymerization at 1 atm ethylene pressure was carried out in a Schlenk tube. Complex **6** was added followed by toluene (30 ml) and then the required amount of co-catalyst introduced by syringe. The solution was then stirred at 30 °C under 1 atm of ethylene pressure. After 30 min, the solution was

quenched with 10% hydrochloric acid in ethanol. The polymer was washed with ethanol, dried under reduced pressure at 40 °C and then weighed.

Ethylene polymerization at 5 / 10 atm ethylene pressure. The polymerization at high ethylene pressure was carried out in stainless steel autoclave (0.25 L) equipped with an ethylene pressure control system, a mechanical stirrer and a temperature controller. At the required reaction temperature, freshly distilled toluene (30 ml) was injected into the autoclave, followed by the complex (2.0 μmol) dissolved in toluene (50 ml). The required amount of co-catalyst (MAO, Et₂AlCl) and more toluene (20 ml) were then injected successively to complete the addition. The autoclave was immediately pressurized to high ethylene pressure and the stirring commenced. After the required reaction time, the ethylene pressure was released and the polymer collected and washed with ethanol. Following drying under reduced pressure at 40 °C, the polymer sample was weighed.

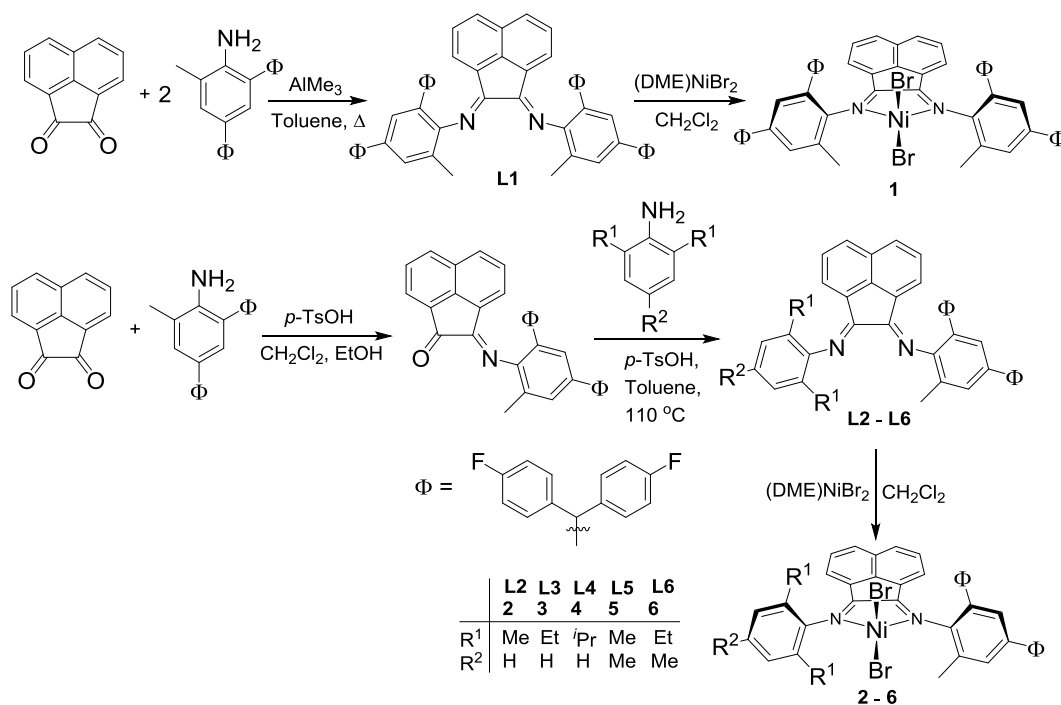
RESULTS AND DISCUSSION

Synthesis and characterization of ligands and complexes

Compound 1,2-[2,4-((4-FC₆H₄)₂CH)₂-6-MeC₆H₄N]₂-C₂C₁₀H₆ (**L1**) was prepared based on a method outlined in a previous procedure,^{10b,15} in which trimethylaluminum was firstly reacted with 2,4-bis[bis(4-fluorophenyl)methyl]-6-methylbenzenamine to generate an aminoalane dimer,^{10b} which could then be further reacted with acenaphthylene-1,2-dione to give **L1** (Scheme 1). By contrast the unsymmetrical counterparts, 1-[2,4-((4-FC₆H₄)₂CH)₂-6-MeC₆H₄N]-2-(ArN)C₂C₁₀H₆ (Ar = 2,6-Me₂C₆H₃ **L2**, 2,6-Et₂C₆H₃ **L3**, 2,6-*i*-Pr₂C₆H₃ **L4**, 2,4,6-Me₃C₆H₂ **L5**, 2,6-Et₂-4-MeC₆H₂ **L6**), were prepared by sequential condensation reactions involving firstly treatment of acenaphthylene-1,2-dione with one molar equivalent of 2,4-bis[bis(4-fluorophenyl)methyl]-6-methylbenzenamine to

give imine-ketone 1,2-2-[2,4-bis(bis(4-fluorophenyl)methyl)-6-methylphenylimino]

acenaphthylen-1-one, which could then be further reacted with the corresponding alkyl-



SCHEME 1. Synthetic procedure for **L1** - **L6** and **1** - **6**.

substituted aniline to give **L2** – **L6** in acceptable yields (Scheme 1). **L1** – **L6** have all been characterized by NMR (¹H, ¹³C) and IR spectroscopy as well as by elemental analysis.

The diiminoacenaphthenes, **L1** – **L6**, were individually treated with an equivalent of (DME)NiBr₂ (DME = 1,2-dimethoxyethane) in dichloromethane to produce the corresponding nickel(II) bromide complexes (**1** – **6**) in good yields (Scheme 1). Complexes **1** – **6** were characterized by FT-IR spectroscopy and elemental analysis. In the FT-IR spectra of **1** – **6**, the ν(C=N) stretching vibration appeared in the range 1620 - 1650 cm⁻¹, whereas in **L1** - **L6** the corresponding band appeared between 1670 and 1640 cm⁻¹; this shift to lower wavenumber being consistent with effective coordination between the nickel ion and the N_{imino} atoms. In addition, **3** and **6** were the subject of single crystal X-ray diffraction studies.

TABLE 2. Selected bond lengths (Å) and angles (°) for **3** and **6**.

	3	6
Distance / Å		
Ni(1)-N(1)	2.023(6)	2.016(4)
Ni(1)-N(2)	2.029(6)	2.041(4)
Ni(1)-Br(1)	2.3397(14)	2.3411(10)
Ni(1)-Br(2)	2.3346(13)	2.3355(9)
N(1)-C(1)	1.271(9)	1.280(6)
N(2)-C(11)	1.315(9)	1.291(6)
N(1)-C(13)	1.469(9)	1.454(6)
N(2)-C(24)	1.426(9)	1.447(6)
Bond angles / °		
N(1)-Ni(1)-N(2)	83.2(2)	82.92(15)
N(1)-Ni(1)-Br(2)	112.71(17)	106.03(12)
N(2)-Ni(1)-Br(2)	106.22(16)	122.40(11)
N(1)-Ni(1)-Br(1)	106.75(18)	115.63(11)
N(2)-Ni(1)-Br(1)	115.37(17)	100.97(12)
Br(1)-Ni(1)-Br(2)	124.94(5)	122.62(3)

Crystals of **3** and **6** suitable for the X-ray determination were grown by the slow diffusion of diethyl ether into the respective dichloromethane solutions. Their molecular structures are shown in Figures 1 and 2; selected bond lengths and angles are listed in Table 2. The structures of **3** and **6** are closely related and will be discussed together. In each case a single nickel center is surrounded by two

nitrogen donors belonging to the diiminoacenaphthene and two bromide ligands to complete a geometry that can be best described as distorted tetrahedral. The Ni1–N1 (2.023(6) (**3**), 2.016(4) Å (**6**)) and Ni1–N2 (2.029(6) (**3**) 2.041(4) Å (**6**)) bond lengths are comparable as are the N1–Ni1–N2 bite angles for the chelating ligands (83.2(2)° (**3**) and 82.92(15)° (**6**)). The N1–C1 and N2–C11 bond distances (range: 1.271(9) – 1.315(9) Å) show typical C=N double-bond character and are significantly shorter than the N1–C13 and N2–C24 distances (range: (1.426(9) – 1.469(9) Å). The N1, N2 and Ni1 plane is almost perpendicular to the *N*-aryl ring linked to N1 (dihedral angle = 85.65° (**3**), 83.15° (**6**)), while to N2 it is more tilted (dihedral angle = 79.26° (**3**), N2 74.02°(**6**)), the latter likely due to the unsymmetrical nature of the 2,6-substitution pattern.

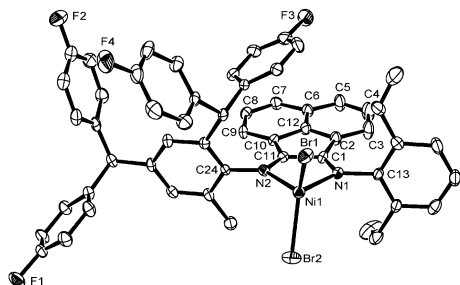


FIGURE 1. ORTEP drawing of **3**. Thermal ellipsoids are shown at the 30% probability level. Hydrogen atoms have been omitted for clarity.

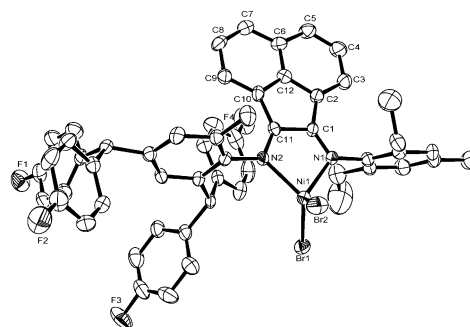


FIGURE 2. ORTEP drawing of **6**. Thermal ellipsoids are shown at the 30% probability level. Hydrogen atoms have been omitted for clarity.

Catalytic evaluation of **1** – **6** in ethylene polymerization

Complex **6** was selected as the test precatalyst and initially screened for the polymerization of ethylene in the presence of five different alkylaluminium co-catalysts namely MAO, MMAO, Et₂AlCl, EtAlCl₂ and Me₂AlCl, under an ethylene pressure of one atmosphere; the results are compiled in Table 3. On inspection of the results, the highest activities were obtained using MAO and Et₂AlCl (entries 1 and 3, Table 3). Hence further detailed catalytic investigations of **1** – **6** were performed using these two co-catalysts.

TABLE 3. Ethylene polymerization by **6** with various co-catalysts at 1 atmosphere of ethylene^a

entry	co-cat	Al/Ni	act ^b	<i>M_w</i> ^c	<i>M_w</i> / <i>M_n</i> ^c	<i>T_m</i> ^d (°C)
1	MAO	2000	6.2	1.62	2.27	51.0
2	MMAO	2000	4.2	1.65	2.13	44.2
3	Et ₂ AlCl	400	6.6	1.11	2.70	65.2
4	EtAlCl ₂	400	3.1	1.07	2.23	57.0
5	Me ₂ AlCl	400	trace			

^aGeneral conditions: 2.0 μmol Ni, 30 mL toluene, 30 min, 30 °C. ^b10⁵ g of PE (mol of Ni)^{−1} h^{−1}. ^cDetermined by GPC, and *M_w*: 10⁵ g mol^{−1}. ^dDetermined by DSC.

TABLE 4. The catalytic evaluation of **1** – **6** activated with MAO^a

entry	pre-cat.	T/°C	t/min	Al/Ni	Act. ^b	M_w ^c	M_w/M_n ^c	T_m ^d (°C)
1	6	20	30	1000	3.98	5.79	3.18	115.6
2	6	20	30	1500	4.90	4.88	3.10	105.6
3	6	20	30	2000	5.46	4.47	3.16	111.8
4	6	20	30	2500	4.16	3.67	3.62	113.8
5	6	20	30	3000	3.56	3.57	3.03	105.6
6	6	30	30	2000	6.89	2.24	3.17	99.5
7	6	40	30	2000	5.15	1.97	2.87	82.2
8	6	50	30	2000	3.85	1.52	2.26	68.1
9	6	60	30	2000	3.02	1.32	2.38	63.1
10	6	70	30	2000	1.58	1.12	2.56	52.5
11	6	30	15	2000	9.12	2.17	3.12	102.4
12	6	30	45	2000	4.82	3.25	3.67	108.4
13	6	30	60	2000	4.50	3.42	2.78	100.6
14 ^e	6	30	30	2000	3.14	2.19	2.57	73.8
15 ^f	6	30	30	2000	0.62	0.62	2.27	51.0
16	1	30	30	2000	6.00	3.42	2.78	118.8
17	2	30	30	2000	8.52	2.62	2.72	85.7
18	3	30	30	2000	8.07	1.38	3.85	97.3
19	4	30	30	2000	6.16	3.18	3.60	99.8
20	5	30	30	2000	7.16	2.07	3.37	95.6

^aConditions: 2.0 μmol of Ni; 100 mL toluene and 10 atm ethylene. ^b 10^6 g of PE (mol of Ni)⁻¹ h⁻¹. ^c M_w : 10^5 g mol⁻¹, M_w and M_w/M_n determined by GPC. ^dDetermined by DSC. ^e5 atm, ^f1 atm.

With the aim to optimize the reaction parameters (*e.g.*, Al/Ni ratio, temperature, reaction duration and pressure), **6** and MAO were firstly evaluated as the precatalyst/co-catalyst combination; the results obtained are assembled in Table 4. On increasing the Al/Ni molar ratio from 1000 to 3000 at 20 °C over a 30 minute run time (entries 1 – 5, Table 4), the optimum activity of 5.46×10^6 g of PE (mol of Ni)⁻¹ h⁻¹ was observed at a Al/Ni molar ratio of 2000 (entry 3, Table 4). At this molar ratio, the reaction temperature was raised from 20 to 70 °C (entries 3 and 6 – 10, Table 4) and the highest activity of 6.89×10^6 g of PE (mol of Ni)⁻¹ h⁻¹ was observed at 30 °C (entry 6, Table 4), after which the activity steadily decreased reaching a minimum of 1.58×10^6 g of PE (mol of Ni)⁻¹ h⁻¹ at 70 °C. Prolonging the reaction time from 15 to 60 minutes resulted in a gradual decrease in activity (entries 3 and 11 – 13, Table 4), suggesting that the active species formed quickly after addition of the MAO and then underwent slow deactivation over time. Furthermore, the reactions conducted at elevated ethylene pressure led to a marked increase in activity (entries 3 and 14 – 15, Table 4); this pressure-activity relationship is consistent with previous observations.^{7c-f}

Using the optimized conditions established for **6**, based on an Al/Ni ratio of 2000, a temperature of 30 °C and a run time of 30 minutes, precatalysts **1** – **5** were also screened for ethylene polymerization (entries 16 – 20, Table 4). All systems displayed good activity and revealed some structure-activity correlation: **5** [2,4,6-tri(Me)] > **6** [2,6-di(Et)-4-Me] as well as **2** [2,4-di(Me)] > **3** [2,6-di(Et)] > **4** [2,6-di(i-Pr)] > **1** [symmetrical bulky substituents]. It would seem apparent that as the steric properties at the *ortho*-positions increase the activity decreases, suggesting that the bulkier substituents hinder the ethylene insertion resulting in lower polymerization rates.^{3b,7b,d,f}

The properties of the polyethylenes obtained using **1** – **6** such as molecular weight, polydispersity and melting point are shown to be dependent on the reaction parameters as well as the nature of the *N*-aryl R¹ and R² substitution pattern. Typically, the molecular weight of the polyethylene falls as the amount of MAO increases (entries 1 – 5, Table 4), which is consistent with previous findings in which high molar ratios of Al/Ni lead to an increased probability of chain transfer from the active nickel species to the aluminium co-catalyst and ultimately termination.¹⁶ A representative set of

GPC curves using precatalyst **6** clearly highlights this trend (Figure 3).

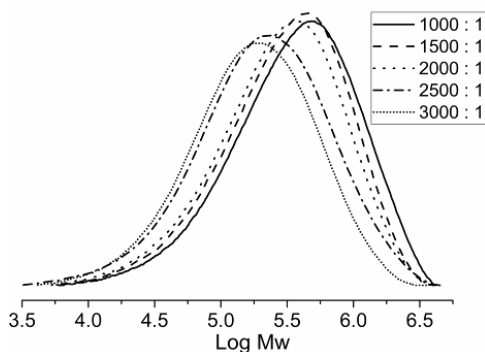


Figure 3. GPC curves for the polyethylenes obtained using **6**/MAO with various Al/Ni ratios (entries 1 – 5, Table 4)

With regard to the effects of temperature on the polymerization, the data reveal that as it increases the polyethylenes display lower molecular weight, narrower polydispersity and lower melting points (entries 3 and 6 – 10, Table 4). This trend is borne out in the variation in the GPC curves generated for the polymers formed using **6**/MAO (Figure 4), which clearly illustrate that a decrease in molecular weight occurs as the reaction temperature rises from 20 to 70 °C; findings that are in agreement with reported Ni α -diimine catalytic systems.^{7,9,16} On the other hand, the GPC curves shown in Figure 5 indicate that as the reaction time is prolonged the molecular weights of the polyethylenes increase.

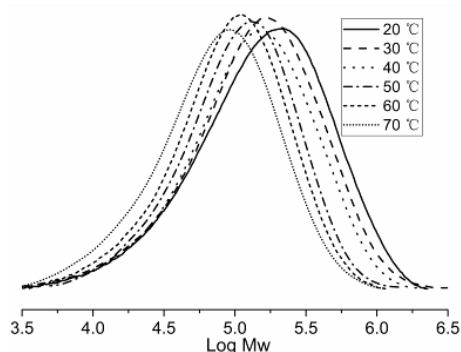


Figure 4. GPC curves for the polyethylenes obtained using **6**/MAO at 20 – 70 °C (entries 3 and 6 – 10, Table 4)

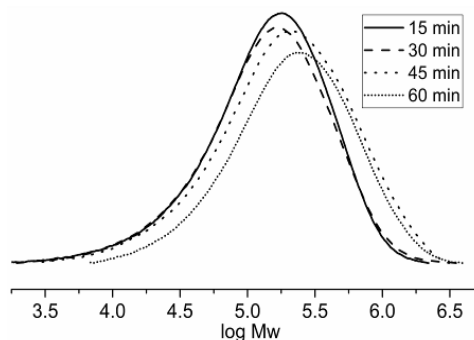


Figure 5. GPC curves for the polyethylenes obtained using **6**/MAO at different reaction times (entries 3 and 11 – 13, Table 4)

Examination of the DSC data shows the melting temperatures (T_m) for the resulting polyethylenes (using **1** – **6**/MAO) to be generally lower than 110 °C, with entry 16 the exception (entries 6 and 16–20, Table 4). This observation is consistent with a high branching content that is likely the result of chain walking occurring with these nickel catalytic systems.^{7,9} The DSC traces for the materials obtained using all six catalysts at 30 °C are depicted in Figure 6.

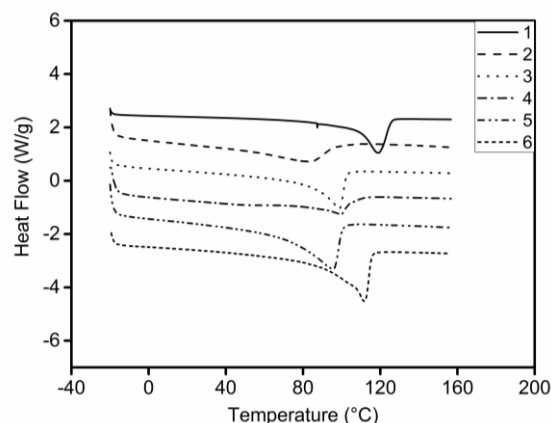


Figure 6. Stacked DSC traces for the polyethylenes obtained using **1** – **6**/MAO at 30 °C (entries 3 and 16 – 20, Table 4)

A representative sample of the polyethylene obtained using **6**/MAO at 30 °C (entry 6, Table 4) was also characterized by ¹³C NMR spectroscopy (Figure 7). Based on previously described methods for interpretation of such spectra,¹⁷ 44 branches in 1000 carbons were determined which include methyl (64.78%),

ethyl (7.55%) and longer chain branches (27.67%).

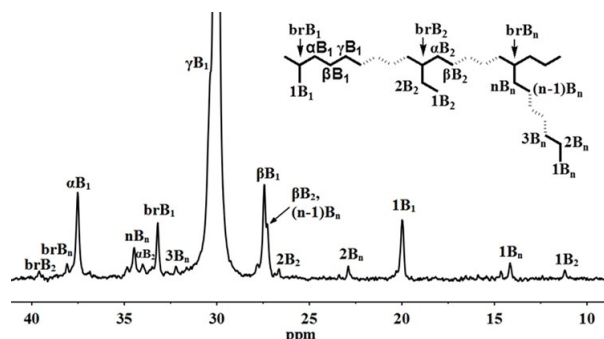


Figure 7. ^{13}C NMR spectrum of the polyethylene obtained using **6**/MAO at 30 °C (entry 6, Table 4)

Precatalyst **6** was again used to ascertain the optimal parameters for the polymerization using diethylaluminium chloride as the co-catalyst; the results are summarized in Table 5.

TABLE 5. The catalytic evaluation of **1** - **6** activated with Et_2AlCl ^a

entry	pre-cat.	T/°C	t/min	Al/Ni	Act. ^b	M_w^c	M_w/M_n^c	T_m^d (°C)
1	6	20	30	200	4.73	5.07	3.69	106.5
2	6	20	30	300	5.29	4.49	4.32	111.5
3	6	20	30	400	5.93	4.40	4.22	108.7
4	6	20	30	500	5.33	3.87	4.22	110.2
5	6	20	30	600	5.00	3.45	4.27	115.4
6	6	30	30	400	7.30	2.99	3.14	100.4
7	6	40	30	400	6.17	2.43	3.41	98.8
8	6	50	30	400	5.30	1.24	2.36	63.7
9	6	60	30	400	4.10	1.18	2.66	62.6
10	6	70	30	400	2.67	0.99	2.98	54.3
11	6	30	15	400	10.2	2.88	3.41	103.2
12	6	30	45	400	5.43	3.34	3.38	99.7
13	6	30	60	400	4.55	3.77	4.11	99.2
14 ^e	6	30	30	400	3.96	2.34	2.90	68.5
15 ^f	6	30	30	400	0.66	1.11	2.70	65.2
16	1	30	30	400	6.03	4.88	3.39	99.1
17	2	30	30	400	7.70	1.59	3.68	103.2
18	3	30	30	400	7.07	3.87	4.27	108.2
19	4	30	30	400	6.83	4.56	3.63	111.5
20	5	30	30	400	7.51	3.68	4.32	104.2

^aConditions: 2.0 μmol of Ni; 100 mL toluene for 10 atm ethylene. ^b 10^6 g of PE (mol of Ni)⁻¹ h⁻¹. ^c M_w : 10^5 g mol⁻¹, M_w and M_w/M_n determined by GPC. ^dDetermined by DSC. ^e5 atm, ^f1 atm.

Generally **6**/ Et_2AlCl , under comparable conditions, displays better activity in ethylene polymerization than that observed using **6**/MAO. In the presence of different Al/Ni molar ratios, ranging from 200 to 600 at 20 °C (entries 1 – 5, Table 5), the highest activity for **6** was achieved at a ratio of 400 [5.93×10^6 g of PE (mol of Ni)⁻¹ h⁻¹]. Inspection of the GPC curves obtained at the different Et_2AlCl ratios (Figure 8) reveals that the molecular weights of the polyethylenes decrease as the molar ratio of co-catalyst increases from 200 to 600 (from 5.07×10^5 g mol⁻¹ down to 3.45×10^5 g mol⁻¹), which can be attributed to the increased likelihood of chain transfer from nickel to the aluminium.

Little variation in the polydispersities of the polyethylenes is apparent over this range.

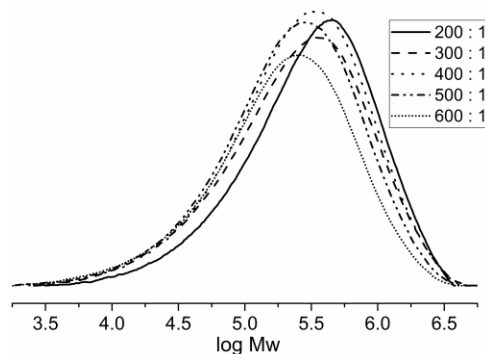


Figure 8. GPC curves for the polyethylenes obtained using **6**/Et₂AlCl with various Al/Ni ratios (entries 1 – 5, Table 5)

With the Al/Ni molar ratio set at 400, the reaction temperature of the polymerization was varied between 20 and 70 °C (entries 3, 6 – 10, Table 5). The maximum activity for **6** of 7.30×10^6 g of PE (mol of Ni)⁻¹ h⁻¹ (entry 6, Table 4) was achieved at 30 °C. On further raising the reaction temperature the activity steadily dropped reaching a minimum at 70 °C (entry 10, Table 5). In comparison with **6**/MAO over the 40 to 70 °C temperature range, **6**/Et₂AlCl displayed superior catalytic performance, indicating better thermal stability of **6** with Et₂AlCl. Moreover, the **6**/Et₂AlCl system still maintained acceptable activity [2.67×10^6 g of PE (mol of Ni)⁻¹ h⁻¹] at an industrial operating temperature of 70 °C (entry 10, Table 5). Characteristically, the polyethylene generated at higher reaction temperature is of lower molecular weight due to the faster decomposition of the active species at elevated temperature. For example, the molecular weight of the polymer obtained at 20 °C is 4.40×10^5 g mol⁻¹ while at 70 °C it drops to 0.99×10^5 g mol⁻¹ (entries 3 and 6 – 10, Table 5); this trend is illustrated in Figure 9.

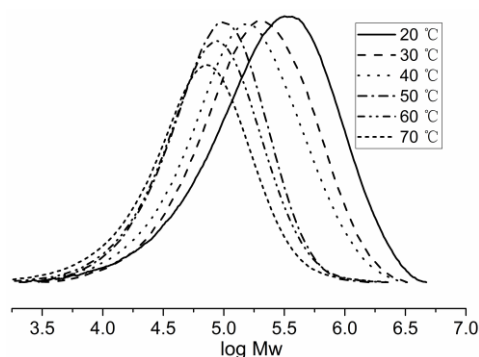


Figure 9. GPC curves for the polyethylenes obtained using **6**/Et₂AlCl at 20 – 70 °C (entries 3, 6 – 10, Table 5)

To investigate the influence of reaction time on catalytic performance, a study was conducted on **6** (at 30 °C; Ni/Al ratio of 400) at 15, 30, 45 and 60 minute time intervals (entries 3, 11 – 13, in Table 5). A peak in activity of 1.02×10^7 g of

PE (mol of Ni)⁻¹ h⁻¹ was observed after 15 minutes which steadily decreased with time reaching the lowest value of 4.55×10^6 g of PE (mol of Ni)⁻¹ h⁻¹ after 60 minutes, as the active species slowly deactivated. By contrast, the molecular weights of the polyethylenes gradually increased over time; their GPC curves are depicted in Figure 10.

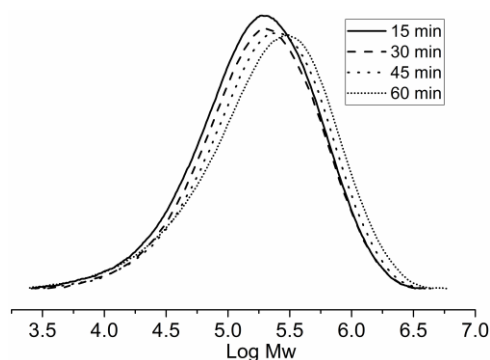


Figure 10. GPC curves for the polyethylenes obtained using **6**/Et₂AlCl at different reaction times (entries 6, 11 – 13, Table 5)

With the conditions fixed at an Al/Ni ratio of 400, the reaction temperature at 30 °C and a run time of 30 minutes, **1** – **5** were all examined for their performance in ethylene polymerization (entries 16 – 20, Table 5). As with the MAO study, the Et₂AlCl-promoted systems displayed similar structure-activity correlations, *i.e.*, the activities decreased as the steric properties were enhanced around the active species. Hence, **5** [2,4,6-tri(Me)] > **6** [2,6-di(Et)-4-Me], and likewise, **2** [2,4-di(Me)] > **3** [2,6-di(Et)] > **4** [2,6-di(*i*-Pr)] > **1** [symmetrical bulky substituents]. While precatalysts **1** [symmetrical bulky substituents] and **4** [2,6-di(*i*-Pr)], bearing the bulkiest *N*-aryl *ortho*-substituents, were at the low end of the activity range, they generated polyethylenes with the highest molecular weights [4.88×10^5 g mol⁻¹ and 4.56×10^5 g mol⁻¹].

In the main, the melting temperatures of the polyethylenes obtained using **1** – **6**/MAO, are slightly higher than those found for **1** – **6**/Et₂AlCl, though still falling lower than 110 °C. Similarly, the relatively low *T_m*'s are indicative of a high

branching content; the DSC curves of the resulting polymers are depicted in Figure 11.

To establish further information on the degree of branching, a sample of the polyethylene obtained using **6**/Et₂AlCl at 30 °C (entry 6,

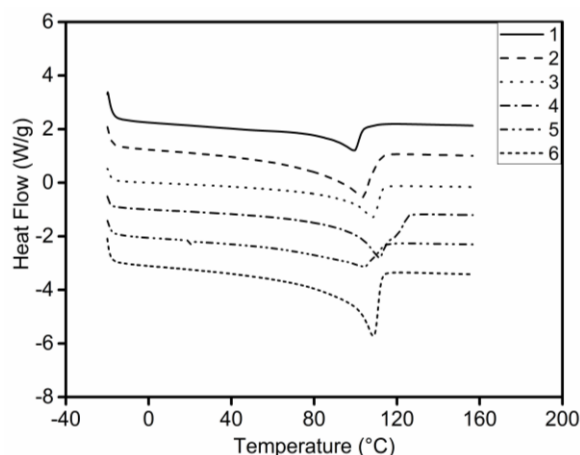


Figure 11. Stacked DSC traces for the polyethylenes obtained using **1** – **6**/Et₂AlCl at 30 °C (entries 3 and 16 – 20, Table 5)

Table 5) was also examined by high temperature ¹³C NMR spectroscopy (Figure 12). The data acquired revealed 38 branches per 1000 carbons including methyl (79.68%), ethyl (10.47%) and longer chain branches (9.85%).

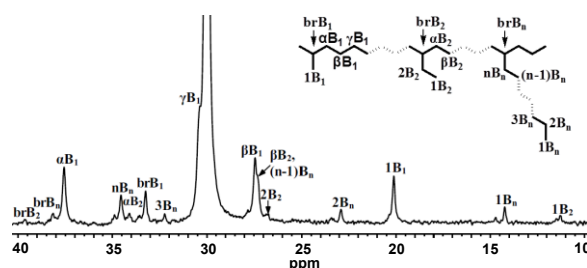


Figure 12. ¹³C NMR spectrum of the polyethylene obtained using **6**/Et₂AlCl at 30 °C (entry 6, Table 5)

TABLE 6. Ethylene polymerization using **1** at elevated temperatures^a

entry	co-cat	T/°C	Al/Ni	Act. ^b	adjusted-act ^c	<i>M_w</i> ^d	<i>M_w</i> / <i>M_n</i> ^d	<i>T_m</i> ^e (°C)
1	MAO	60	2000	4.26	4.97	2.77	2.55	64.4
2	MAO	70	2000	3.87	5.07	2.45	2.57	62.3
3	MAO	80	2000	3.16	4.59	2.30	2.58	51.5
4	MAO	90	2000	1.37	2.20	2.12	2.06	51.8
5	MAO	100	2000	trace	---	---	---	---
6	Et ₂ AlCl	60	400	3.96	4.62	3.01	2.79	63.5
7	Et ₂ AlCl	70	400	3.65	4.78	2.64	2.50	64.2
8	Et ₂ AlCl	80	400	3.44	5.00	2.16	2.49	67.5
9	Et ₂ AlCl	90	400	3.18	5.11	1.85	2.52	58.9
10	Et ₂ AlCl	100	400	1.12	1.98	1.12	2.37	47.2

^aConditions: 2.0 μmol Ni, 100 mL toluene, 30 min, 10 atm ethylene. ^b10⁶ g of PE (mol of Ni)⁻¹ h⁻¹. ^c10⁶ g of PE (mol of Ni)⁻¹ h⁻¹ C_{ethylene}⁻¹. ^dDetermined by GPC, and *M_w* × 10⁵ g mol⁻¹. ^eDetermined by DSC.

Using **1**/MAO and **1**/Et₂AlCl at elevated temperature

Employing the optimal conditions identified using MAO and Et₂AlCl (*vide supra*), precatalyst **1**, incorporating two sterically bulky *N*-2,4-bis(difluorobenzyl)phenyl groups, was investigated in the polymerization of ethylene at reaction temperatures in the range 60 to 100 °C; the results are summarized in Table 6.

Given the lower solubility of ethylene in toluene at higher temperature, the adjusted activities were determined through calculating the

ethylene concentrations at different reaction temperatures (C_{ethylene}, mol L⁻¹ atm⁻¹, Table 6).¹⁸ On activation with MAO, **1** maintained good activity [greater than 3.16 × 10⁶ g of PE (mol of Ni)⁻¹ h⁻¹] at temperatures between 60 and 80 °C. On further raising the reaction temperature to 90 °C, the activity sharply decreased down to 1.37 × 10⁶ g of PE (mol of Ni)⁻¹ h⁻¹. When the temperature reached 100 °C, only trace amounts of polyethylene were obtained. The molecular weights gradually drop as the temperature is raised but nevertheless even at high temperature (60 – 90 °C), **1**/MAO generates polyethylenes with high molecular weights of over 2.12 × 10⁵ g mol⁻¹. Furthermore,

a narrow molecular weight distribution is a feature of all the polyethylenes obtained in this temperature range. The GPC curves in Figure 13 highlight this temperature dependency of the polymer molecular weights (entries 1 – 4, Table 6).

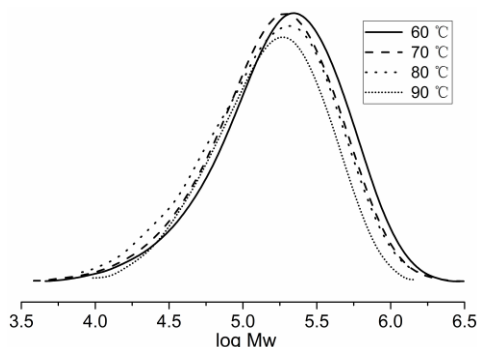


Figure 13. GPC curves for the polyethylenes obtained by the **1**/MAO at 60 – 90 °C (entries 1 – 4, Table 6)

Compared with **1**/MAO, **1**/Et₂AlCl exhibited higher activity and better thermal stability. As the reaction temperature was raised from 60 to 90 °C, the catalytic activities maintained an impressively high level ranging from 3.96×10^6 g of PE (mol of Ni)^{−1} h^{−1} at 60 °C down to 3.18×10^6 g of PE (mol of Ni)^{−1} h^{−1} at 90 °C. Even at temperatures up to 100 °C, the **1**/Et₂AlCl still maintained a remarkable activity of 1.12×10^6 g of PE (mol of Ni)^{−1} h^{−1}. With regard to the properties of the resultant polyethylenes, the GPC curves (Figure 14) highlight the tendency of the molecular weights to decrease as the reaction temperature was increased from 60 to 100 °C (entries 6 – 10, Table 6). The decreased yields of polyethylenes and the lowering of the molecular weights are mainly ascribed to a combination of increased chain transfer relative to chain propagation and to a decreased solubility of ethylene in toluene at elevated temperatures.^{3b,18}

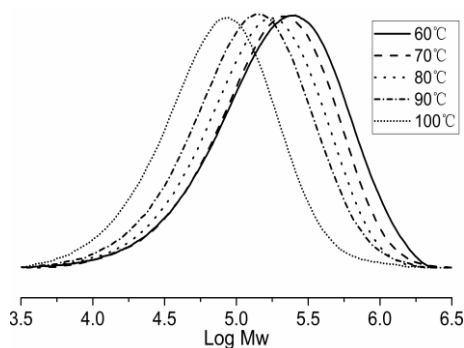


Figure 14. GPC curves for the polyethylenes obtained using **1**/Et₂AlCl at 60 – 100 °C (entries 6 – 10, Table 6)

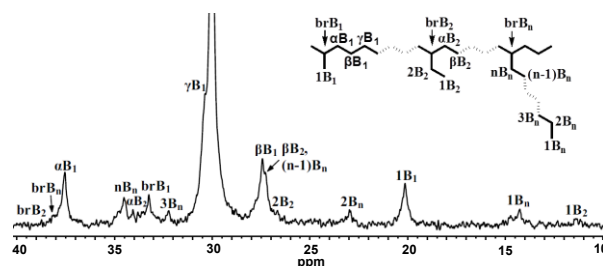


Figure 15. ¹³C NMR spectrum of the polyethylene obtained using **1**/Et₂AlCl at 100 °C (entry 10, Table 5)

According to the DSC data, the melting temperatures for all polyethylenes are relatively low (47.2 – 67.5 °C), suggesting that the polyethylenes are highly branched. This was corroborated in the case of a polyethylene sample obtained at 100 °C (entry 10, Table 6), in which a high temperature ¹³C NMR spectrum (Figure 15) showed there to be 100 branches in 1000 carbons, including methyl (68.11%), ethyl (10.63%) and longer chain branches (21.26%).

In comparison with literature reports and in particular the Ni α -diimine catalysts (see **A** in Chart 1) disclosed by Long and co-workers, which feature a 2,6-substituted pattern for the benzhydryl groups,^{10a,10b} **1**/Et₂AlCl has been shown to display superior thermal stability (up to 100 °C) whilst maintaining high activity. Indeed, **1**/Et₂AlCl exhibited improved catalytic activity and better thermal stability at any comparable temperature. Hence we have shown that by placing only one benzhydryl substituent at the *ortho*-positions of each *N*-aryl

ring, we can increase the capacity of the ethylene monomer to insert into the Ni-C/H bond of the active species. At the same time we have demonstrated that the presence of just the one benzhydryl group per *N*-aryl group is sufficient to block the axial positions of the metal center and slow down the potential catalyst decomposition pathways.^{1a,3b} Likewise, *N*-aryl rotations in the *N,N*-ligand, which would otherwise result in the formation of agostic interactions between the nickel center and the hydrogen atoms within the ligand, are restricted.¹⁹ Overall, **1**/Et₂AlCl has demonstrated an excellent balance between activity and thermal stability, which is mainly attributed to the use of 2,4-bis(difluorobenzhydryl)-6-methylphenyl as the *N*-aryl groups within the α -diimine ligand framework.

CONCLUSIONS

Routes to a series of unsymmetrical and symmetrical diaryliminoacenaphthenes containing either one (**L2** – **L6**) or two (**L1**) *N*-2,4-bis(bis(4-fluorophenyl)methyl)-6-methylphenyl groups have been devised and implemented. Complexation with nickel(II) bromide proceeded smoothly to give **1** – **6**. The molecular structures of **3** and **6** were determined crystallographically and confirm the expected distorted tetrahedral geometry at the nickel center. Upon activation with either MAO or Et₂AlCl, **1** – **6** all exhibit high activities towards ethylene polymerization, generating branched polyethylenes with moderate molecular weights and narrow polydispersities. **1**/Et₂AlCl possessed exceptional thermal stability with an activity up to 1.12×10^6 g of PE (mol of Ni)⁻¹ h⁻¹ even at 100 °C generating high molecular weight (up to 10^5 g mol⁻¹) and highly branched polyethylene. Significantly, **1**/Et₂AlCl represents the most thermally stable, but highly active, Ni α -diimine catalyst for ethylene polymerization reported to date.

ACKNOWLEDGEMENTS

This work is supported by National Natural Science Foundation of China (Nos. 21374123

and U1362204). Natural Science Foundation of Ningbo (2015A610261), and the Research Project Foundation of Zhejiang Educational Department (Y201534705). GAS is grateful to the Chinese Academy of Sciences for a Visiting Scientist Fellowship.

REFERENCES AND NOTES

- a) L. K. Johnson, C. M. Killian, M. Brookhart, *J. Am. Chem. Soc.*, **1995**, *117*, 6414–6415; b) C. M. Killian, D. J. Tempel, L. K. Johnson, M. Brookhart, *J. Am. Chem. Soc.*, **1996**, *118*, 11664–11665.
- a) V. C. Gibson, C. Redshaw, G. A. Solan, *Chem. Rev.*, **2007**, *107*, 1745–1776; b) W.-H. Sun, S. Zhang, W. Zuo, *C. R. Chim.*, **2008**, *11*, 307–316; c) C. Bianchini, G. Giambastiani, L. Luconi, A. Meli, *Coord. Chem. Rev.*, **2010**, *254*, 431–455; d) T. Xiao, W. Zhang, J. Lai, W.-H. Sun, *C. R. Chim.*, **2011**, *14*, 851–855; e) W.-H. Sun, *Adv. Polym. Sci.*, **2013**, *258*, 163–178; f) W. Zhang, W.-H. Sun, C. Redshaw, *Dalton Trans.*, **2013**, *42*, 8988–8997; g) J. Ma, C. Feng, S. Wang, K.-Q. Zhao, W.-H. Sun, C. Redshaw, G. A. Solan, *Inorg. Chem. Front.*, **2014**, *1*, 14–34; h) Z. Flisak, W.-H. Sun, *ACS Catal.*, **2015**, *5*, 4713–4724; i) V. C. Gibson, G. A. Solan, in *Catalysis without Precious Metals*, ed. M. Bullock, Wiley-VCH, Weinheim, **2010**, pp. 111–141; j) V. C. Gibson, G. A. Solan, *Top. Organomet. Chem.*, **2009**, *26*, 107–158.
- a) T. Xie, K. B. McAuley, J. C. C. Hsu, D. W. Bacon, *Ind. Eng. Chem. Res.*, **1994**, *33*, 449–479; b) D. P. Gates, S. A. Svejda, E. Oñate, C. M. Killian, L. K. Johnson, P. S. White, M. Brookhart, *Macromolecules*, **2000**, *33*, 2320–2334.
- a) D. H. Camacho, E. V. Salo, J. W. Ziller, Z. B. Guan, *Angew. Chem., Int. Ed.* **2004**, *43*, 1821–1825; b) C. Popeney, Z.-B. Guan, *Organometallics*, **2005**, *24*, 1145–1155; c) C. S. Popeney, A. L. Rheingold, Z. Guan, *Organometallics*, **2009**, *28*, 4452–4463.
- a) J. Liu, D. Chen, H. Wu, Z. Xiao, H.-Y. Gao, F.-M. Zhu, Q. Wu, *Macromolecules*, **2009**, *42*, 7789–7796; b) H.-Y. Gao, H. B. Hu, F. M. Zhu, Q. Wu, *Chem. Commun.*, **2012**, *48*, 3312–

- 3314; c) F.-S. Liu, H.-B. Hu, Y. Hu, L.-H. Guo, S.-B. Zai, K.-M. Song, H.-Y. Gao, L. Zhang, F.-M. Zhu, Q. Wu, *Macromolecules*, **2014**, *47*, 3325–3331.
6. a) J. Yu, H. Liu, W. Zhang, X. Hao, W.-H. Sun, *Chem. Commun.*, **2011**, *47*, 3257–3259; b) W. Zhao, J. Yu, S. Song, W. Yang, H. Liu, X. Hao, C. Redshaw, W.-H. Sun, *Polymer*, **2012**, *53*, 130–137; c) J. Lai, W. Zhao, W. Yang, C. Redshaw, T. Liang, Y. Liu, W.-H. Sun, *Polym. Chem.*, **2012**, *3*, 787–793; d) X. Cao, F. He, W. Zhao, Z. Cai, X. Hao, T. Shiono, C. Redshaw, W.-H. Sun, *Polymer* **2012**, *53*, 1870–1880; e) W.-H. Sun, W. Zhao, J. Yu, W. Zhang, X. Hao, C. Redshaw, *Macromol. Chem. Phys.*, **2012**, *213*, 1266–1273; f) S. Wang, B. Li, T. Liang, C. Redshaw, Y. Li, W.-H. Sun, *Dalton Trans.*, **2013**, *42*, 9188–9197; g) W. Zhang, S. Wang, S. Du, C.-Y. Guo, X. Hao, W.-H. Sun, *Macromol. Chem. Phys.*, **2014**, *215*, 1797–1809.
7. a) H. Liu, W. Zhao, X. Hao, C. Redshaw, W. Huang, W.-H. Sun, *Organometallics*, **2011**, *30*, 2418–2424; b) H. Liu, W. Zhao, J. Yu, W. Yang, X. Hao, C. Redshaw, L. Chen, W.-H. Sun, *Catal. Sci. Technol.*, **2012**, *2*, 415–422; c) S. Kong, C.-Y. Guo, W. Yang, L. Wang, W.-H. Sun, R. Glaser, *J. Organomet. Chem.*, **2013**, *725*, 37–45; d) C. Wen, S. Yuan, Q. Shi, E. Yue, D. Liu, W.-H. Sun, *Organometallics*, **2014**, *33*, 7223–7231; e) L. Fan, S. Du, C.-Y. Guo, X. Hao, W.-H. Sun, *J. Polym. Sci. Part A: Polym. Chem.*, **2015**, *53*, 1369–1378; f) S. Du, Q. Xing, Z. Flisak, E. Yue, Y. Sun, W.-H. Sun, *Dalton Trans.*, **2015**, *44*, 12282–12291; g) S. Du, S. Kong, Q. Shi, J. Mao, C.-Y. Guo, J. Yi, T. Liang, W.-H. Sun, *Organometallics*, **2015**, *34*, 582–590; h) L. Fan, E. Yue, S. Du, C.-Y. Guo, X. Hao, W.-H. Sun, *RSC Adv.*, **2015**, *5*, 93274–93282.
8. a) W.-H. Sun, S. Song, B. Li, C. Redshaw, X. Hao, Y. Li, F. Wang, *Dalton Trans.*, **2012**, *41*, 11999–12010; b) J. Lai, X. Hou, Y. Liu, C.; Redshaw, W.-H. Sun, *J. Organomet. Chem.*, **2012**, *702*, 52–58; c) X. Hou, Z. Cai, X. Chen, L. Wang, C. Redshaw, W.-H. Sun, *Dalton Trans.*, **2012**, *41*, 1617–1623; d) X. Hou, T. Liang, W.-H. Sun, C. Redshaw, X. Chen, *J. Organomet. Chem.*, **2012**, *708–709*, 98–105; e) E. Yue, L. Zhang, Q. Xing, X. Cao, X. Hao, C. Redshaw, W.-H. Sun, *Dalton Trans.*, **2014**, *43*, 423–431; f) E. Yue, Q. Xing, L. Zhang, Q. Shi, X.-P. Cao, L. Wang, C. Redshaw, W.-H. Sun, *Dalton Trans.*, **2014**, *43*, 3339–3346.
9. a) D. Jia, W. Zhang, W. Liu, L. Wang, C. Redshaw, W.-H. Sun, *Catal. Sci. Technol.*, **2013**, *3*, 2737–2745; b) Q. Liu, W. Zhang, D. Jia, X. Hao, C. Redshaw, W.-H. Sun, *Appl. Catal. A: Gen.*, **2014**, *475*, 195–202; c) M. Gao, S. Du, Q. Ban, Q. Xing, W.-H. Sun, *J. Organomet. Chem.*, **2015**, *798*, 401–407.
10. a) J. L. Rhinehart, L. A. Brown, B. K. Long, *J. Am. Chem. Soc.*, **2013**, *135*, 16316–16319; b) J. L. Rhinehart, N. E. Mitchell, B. K. Long, *ACS Catal.*, **2014**, *4*, 2501–2504; c) S. Dai, X. Sui, C. Chen, *Angew. Chem. Int. Ed.*, **2015**, *54*, 9948–9953.
11. a) D. Guo, L. Han, T. Zhang, W.-H. Sun, T. Li, X. Yang, *Macromol Theory Simul.*, **2002**, *11*, 1006–1012; b) T. Zhang, D. Guo, S. Jie, W.-H. Sun, T. Li, X. Yang, *J. Polym. Sci., Part A: Polym. Chem.*, **2004**, *42*, 4765–4774; c) T. Zhang, W.-H. Sun, T. Li, X. Yang, *J. Mol. Catal. A: Chem.*, **2004**, *218*, 119–124; d) W. Yang, Y. Chen, W.-H. Sun, *Macromol. Chem. Phys.*, **2014**, *215*, 1810–1817.
12. X. Wang, L. Fan, Y. Yuan, S. Dub, Y. Sun, G. A. Solan, C.-Y. Guo, W.-H. Sun, *Dalton Trans.*, **2016**, *45*, 18313–18323.
13. G. M. Sheldrick, SHELXTL-97, Program for the Refinement of Crystal Structures; University of Gottingen: Göttingen, Germany, **1997**.
14. A. L. Spek, *Acta Crystallogr.*, **2009**, *D65*, 148–155.
15. a) J. C. Gordon, P. Shukla, A. H. Cowley, J. N. Jones, D. W. Keogh, B. L. Scott, *Chem. Commun.*, **2002**, *22*, 2710–2711; b) P. Shukla, A. H. Cowley, J. N. Jones, J. C. Gordon, B. L. Scott, *Dalton Trans.*, **2005**, 1019–1022.
16. a) S. A. Svejda, M. Brookhart, *Organometallics*, **1999**, *18*, 65–74; b) G. J. P. Britovsek, M. Bruce, V. C. Gibson, B. S. Kimberley, P. J. Maddox, S. Mastroianni, S. J. McTavish, C. Redshaw, G. A. Solan, S. Stromberg, A. J. P. White, D. J. Williams, *J. Am. Chem. Soc.*, **1999**, *121*, 8728–8740; c) M.

- Helldörfer, W. Milius, H. G. Alt, *Inorg. Chim. Acta*, **2003**, 351, 34–42; d) G. J. P. Britovsek, S. A. Cohen, V. C. Gibson, M. V. Meurs, *J. Am. Chem. Soc.*, **2004**, 126, 10701–10712; e) B. K. Bahuleyan, G. W. Son, D.-W. Park, C.-S. Ha, I. Kim, *J. Polym. Sci., Part A: Polym. Chem.*, **2008**, 46, 1066–1082.
17. G. B. Galland, R. F. de Souza, R. S. Mauler, F. F. Nunes, *Macromolecules*, **1999**, 32, 1620–1625.
18. a) W. Krauss, W. Gestrich, *Chem.-Technol.*, **1977**, 6, 513; b) L. S. Lee, H. J. Ou, H. F. Hsu, *Fluid Phase Equilib.*, **2005**, 231, 221–230.
19. D. J. Tempel, L. K. Johnson, R. L. Huff, P. S. White, M. Brookhart, *J. Am. Chem. Soc.*, **2000**, 122, 6686–6700.

GRAPHICAL ABSTRACT

YANJUN CHEN, SHIZHEN DU, CHUANBING HUANG, GREGORY A. SOLAN, XIANG HAO AND WEN-HUA SUN

**Balancing High Thermal Stability with High Activity in
Diaryliminoacenaphthene-Nickel(II) Catalysts for Ethylene Polymerization**

N,N-Diaryliminoacenaphthene-nickel(II) bromide complexes, on activation with MAO or Et₂AlCl, display outstanding activity towards ethylene polymerization (up to 1.02×10^7 g of PE (mol of Ni)⁻¹ h⁻¹), exceptional thermal stability and generate high molecular weight branched polyethylene at temperatures as high as 100 °C.

